The Role of Mg in Void Formation during Plastic Deformation of AA6016 Aluminium Alloys

O. León-García[1], R. Petrov[2], L.A.I. Kestens[2, 3]
[1]*Materials Innovation Institute, Mekelweg 2, 2628 CD Delft, The Netherlands;*
[2]*Ghent University, Technologiepark 903, Ghent 9052, Belgium;*
[3]*Delft University of Technology, Mekelweg 2, 2628 CD Delft, The Netherlands;*
E-mail: *LeonGarcia@m2i.nl*

Abstract
The fracture behaviour of two AA6016 aluminium alloys with different magnesium content was studied after uniaxial tensile tests. SEM fractographs of both materials suggest two types of failure mechanisms. The first is characterized by a sequence of events, i.e. void initiation, growth and coalescence on constituent particles, whereas the second one can be identified as ductile intergranular failure. The second type of failure is observed more often in the aluminium alloy with higher magnesium content. In both aluminium alloys, secondary cracks were found close to the fracture surface on the cross-section plane of the tensile sample. Orientation contrast microscopy images show that the secondary cracks were formed either by an intergranular failure mechanism or by local plastic instabilities such as shear bands which subsequently progress into cracks. The higher magnesium content gives higher strength but reduces the ductility by weakening the grain boundaries.

Keywords: Intergranular ductile failure, AA6016 aluminium alloys, void initiation, EBSD

1. Introduction

The 6XXX aluminium sheet alloys are introduced in the automotive industry as a potential solution for weight reduction. One example for their application is the outer panels of cars [1], where the formability is an important issue but it is limited by plastic instabilities and failure. Thus, the understanding of failure mechanisms and ensuing control could lead to the improvement in fracture resistance of these aluminium alloys.

From a microstructural point of view, the fracture of this aluminium alloy series could occur in an intergranular [2-4] or transgranular [4-7] mode. The former mode has been attempted to be avoided because it causes low ductility and fracture toughness. The reason for the intergranular ductile failure of aluminium alloys has been mainly attributed to the presence of particles along grain boundaries or to the existence of a soft region close to grain boundaries known as a precipitation free zone which possibly acts as a deformation localization site. In the case of the former instance, the variety of particles reported to induce intergranular fracture can be precipitates, dispersoids or impurities as sodium, calcium and strontium [3].

In the case of the transgranular ductile failure of aluminium alloys, particularly the AA6XXX series, the failure micromechanisms are usually a sequence of void nucleation, growth and final coalescence of coarse second phase particles. These particles are often constituents with size larger than 1 μm, mainly Fe-containing intermetallics, which have been reported to have a detrimental effect on the mechanical properties [9]. In the case of ductile failure, the brittleness of these intermetallics and their weak adhesion to the Al matrix turned them into suitable sites for void nucleation which can be initiated at even relatively low strains [6].
However, a combination of both failure behaviours is often found in aluminium alloys in certain conditions. The microstructural variables which affect the transition from transgranular to intergranular failure have been reported to be the size of the precipitate free zone [10], the distribution of coarse particles, the slip band spacing during deformation [2, 4] and the segregation of precipitates or trace impurities [3] along grain boundaries.
The AA6XXX aluminium alloy series are heat treatable and their higher strength is based on precipitation hardening of Mg-Si precipitates. The influence of magnesium on the strength of these aluminium alloys was studied by Caceres et al. [8] on as-cast conditions where increasing the amount of magnesium leads to higher tensile strength but reduces the elongation at fracture.
The objective of the present study is to analyse the origin of void nucleation of two AA6016 aluminium alloys with different magnesium content subjected to tensile deformation. Fractography studies together with the use of electron back-scatter diffraction (EBSD) technique on the cross-section of tensile samples were used to clarify the mechanisms by which void initiation occurs.

2. Experimental procedure

The material used in this study consisted of two different variants of AA6016 aluminium alloys of which the principal difference is in the magnesium content: one containing 0.4 wt% Mg, referred to as type 4Mg, and the other one with 0.6 wt% Mg, i.e. type 6Mg. Both alloys were in overaged condition. The microstructure of both alloys is formed by a similar population of plate-like constituents (equivalent diameter of 4 μm) embedded in a recrystallized aluminium matrix. These constituents were recognized as α-AlFeMnSi and β-AlFeSi and their area fraction in both alloys is around 1%. The grain shape of the aluminium matrix is similar for both alloys but with a small difference in size. The grain intercept length along rolling direction is 35.2 ± 5.9 μm and 41.2 ± 7.2 μm for types 6Mg and 4Mg, respectively.
Uniaxial tensile tests on both aluminium alloys were made on sheet-type specimens with a gauge length of 25 mm and a width of 6 mm; following the standard ASTM E 8M [12]. The samples were cut from the sheet by an electro-discharge machining equipment. The tensile axis of the samples was oriented parallel to the sheet rolling direction. Three samples were tested for each material type at a constant crosshead displacement rate of 10 mm/min, which corresponds to a strain rate of 0.0045 s^{-1}. The fracture surface of the broken samples was analyzed by scanning electron microscopy (SEM).

The cross-section of the broken tensile specimens was afterwards prepared for SEM observation and crystal orientation mapping by EBSD technique. The plane for observation was chosen to be perpendicular to the sample TD, i.e. the RD-ND plane. The samples were mechanically polished using UPS as final polishing step in order to minimize both particle detachment from the matrix and rounding the fracture edges which would possibly be produced by electropolishing. The equipment employed for EBSD analysis was a FEI XL30 type environmental SEM with an LaB_6 filament equipped with an EDAX/TSL OIM system. The crystal orientation maps were made with a step size of 100 nm and a square scan grid.

3. Experimental results

3.1 Tensile properties and SEM-fractography

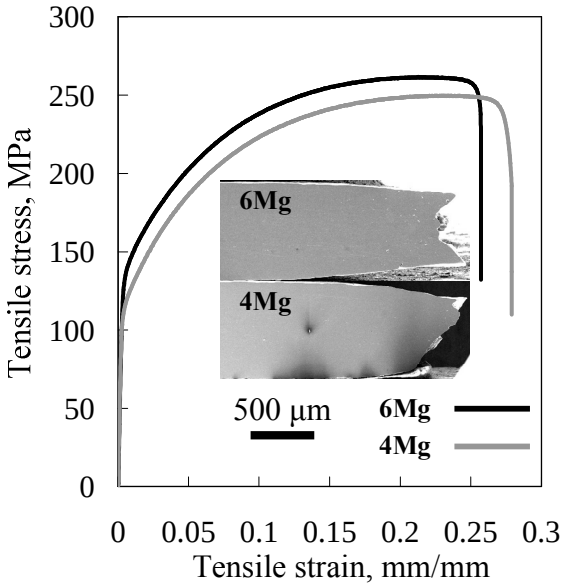

Figure 1. Tensile stress-strain curve

The engineering stress-strain curves for alloys containing 0.6 (Type 6Mg) and 0.4 (type 4Mg) %Mg are shown in Figure 1 while Table 1 summarizes the mechanical properties of both alloys. As was expected [8], the aluminium alloy with the higher magnesium content, type 6Mg, showed a higher ultimate strength of approximately 16 MPa whereas the elongation at fracture was inferior compared to the type 4Mg alloy. The Vickers microhardness shows the same tendency. The reason is attributed to the strengthening of the aluminium matrix where the alloy with higher magnesium content is assumed to create more hardening precipitation particles. In the case of the strain-hardening exponent, the values are similar although the type 4Mg alloy shows a slightly higher value.

Table 1 Tensile properties and microhardness of both AA6016 alloys.

	Type 6Mg	Type 4Mg
Ultimate stress, MPa	262.7	246.6
Elongation at fracture, %	26.09	27.74
Strain-hardening exponent, n ($\sigma=K\varepsilon^n$)	0.328	0.344
Strength coefficient K, MPa	569.83	541.99
Vickers microhardness, HV_{300}	93.76	74.66

The deformation and failure mechanisms act in three stages as follows. During tensile tests, the deformation of the samples occurs uniformly along the gauge length *(i)* until the ultimate tensile strength is achieved and the deformation begins to localize *(ii)*, which finally ends with fracture *(iii)*. SEM-fractographs from the broken samples of both aluminium alloys reveal the existence of two different fracture surfaces (cf. Fig. 2). The features appearing in Fig. 2a are characteristic for one of the fracture surface cases observed often in sample 6Mg. Their main characteristic is the polyhedral shapes of which the size is similar to the grain size of the material. The polyhedral facets show traces of shallow dimples which are generally smaller than 1 μm. This type of fracture surface is usually considered as intergranular ductile failure where the plastic deformation occurs before grain boundary decohesion takes place. The shallow dimples suggest the presence of small void initiation sites at grain boundaries, possibly caused by small particles. Another fracture surface observed in some regions of the samples shows a typical ductile failure based on initiation, growth and coalescence of voids. The intermetallic particles are often found to be responsible for void initiation in sample 4Mg (Fig. 2b) and even some of these particles remain in the bottom of the deeper dimples. In several cases, shallower dimple populations are located on the border of the deep dimples which are assumed to be the product of void sheet coalescence. Both types of fracture surfaces appear in both materials although the alloy type 6Mg qualitatively exhibits more zones similar to Figure 2a than alloy type 4Mg.

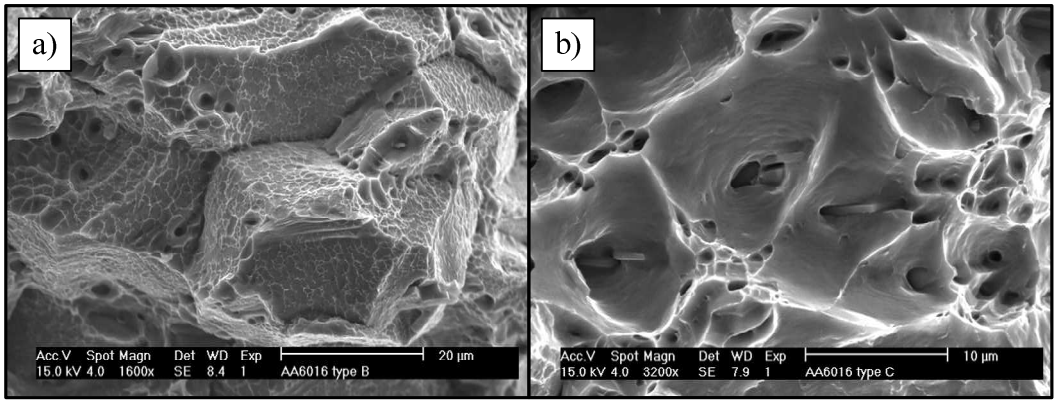

Figure 2. SEM fractographs of broken tensile specimens where ND is oriented vertically. (a) Alloy 6Mg displaying a polyhedrical fracture surface with shallow marks of plastic deformation on these surfaces. These features are characteristic of intergranular ductile failure (b) Alloy 4Mg with a representative zone where void initiation, growth and coalescence on constituent particles is observed. The constituent particles can still be observed in some dimples.

3.2 Damage micro-mechanisms observed in the cross-section

SEM observation of the samples cross-section was made on two regions; one in the zone away from the fracture edge where uniform deformation is assumed and one close to the fracture edge. In the uniform deformation region of both alloys, voids are commonly initiated by either particle-matrix decohesion *(i)* or particle fragmentation *(ii)*. In the first case, the nucleated voids are oriented along the tensile axis with a thickness equal to the thickness of the particle. The voids can

be located on one or both sides of the particle. In case of fragmentation, the particle is split in two or more parts. Some voids are also observed without any particles around. It is believed, however, that the metallographic preparation was responsible for removing the particles from these voids. Not all particles initiate voids and particularly noteworthy is the fact that the large particles are more prone to initiate voids than small particles, as can be observed in the SEM micrographs of Fig. 3. In this region of uniform deformation, both alloys show no appreciable difference in the void formation mechanisms.

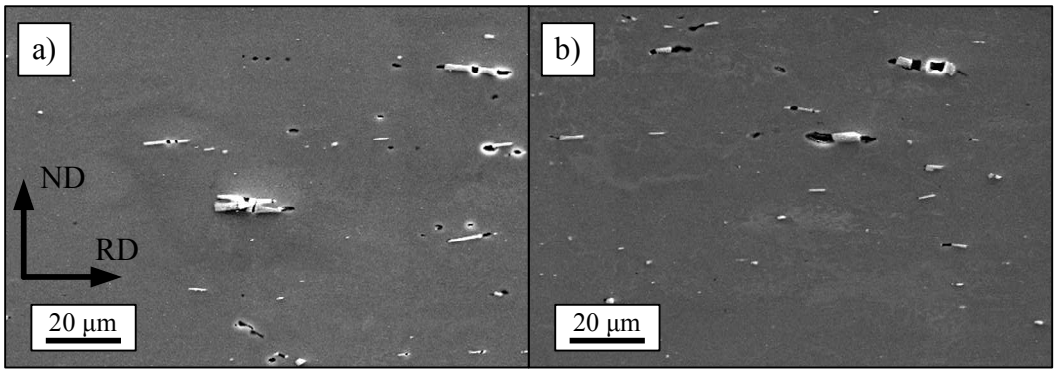

Figure 3. SEM micrographs of broken tensile specimens made in the uniform elongation zone of aluminium alloy type 6Mg (a) and 4Mg (b). In both alloys, the constituent particles are observed to be fragmented or debonded from the matrix. Also voids without particle in the vicinity are observed.

In the region close to the fracture edge of both aluminium alloys, another form of void initiation is observed, which is referred to as cracks due to geometry. These cracks are roughly oriented at 45° with respect to the tensile direction and they can be observed either with or without constituent particles. Some examples are shown in Fig. 4. Based on optical micrographs, 11 cracks were counted close to the fracture edge in one of the tensile specimens of type 6Mg, while only 3 cracks were found in type 4Mg. In the former case, the further crack was localized 825 µm away from the fracture edge while the maximum distance from the fracture edge in the case of 4Mg was 545 µm.

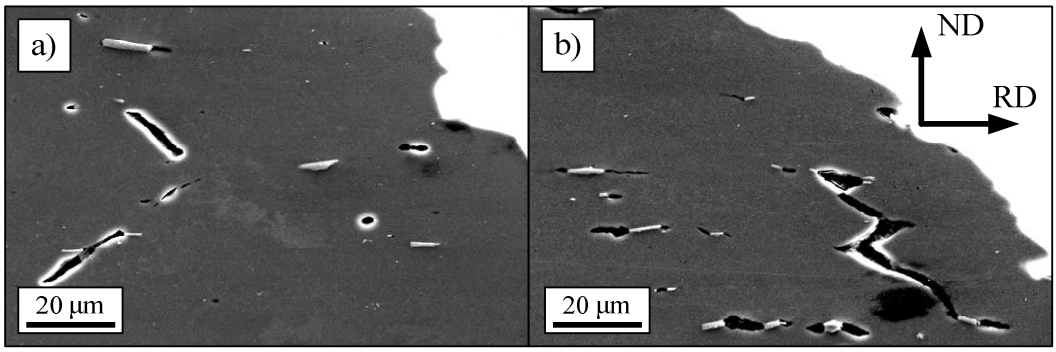

Figure 4. SEM micrographs of broken tensile specimens close to the fracture surface of alloys type 6Mg (a) and 4Mg (b). In the case of (b), the cracks are extended following the constituent particles.

3.3 EBSD analysis

The nature of some cracks and voids was investigated in both alloys by EBSD technique. Fig. 5 illustrates two cases of cracks located close to the fracture edge of 6Mg alloy. In one of the cases (Fig. 5a and b), two cracks are observed along the grain boundaries. The biggest crack, crack 1, is located in the grain boundary of 3 grains, 2 grains from one side and 1 grain from the other side. The misorientation angles between grain 1 and 2 is 35.4° and between grain 1 and 3 is 55.1°. The average crystal orientation of grains 1, 2 and 3 was used for the above measurement. The cracks in the grain boundary formed between grain 1 and 2 are thicker, which allows assuming that the crack initiates in the grain boundary 1-2 and further propagates to the boundary of grains 1 and 3.

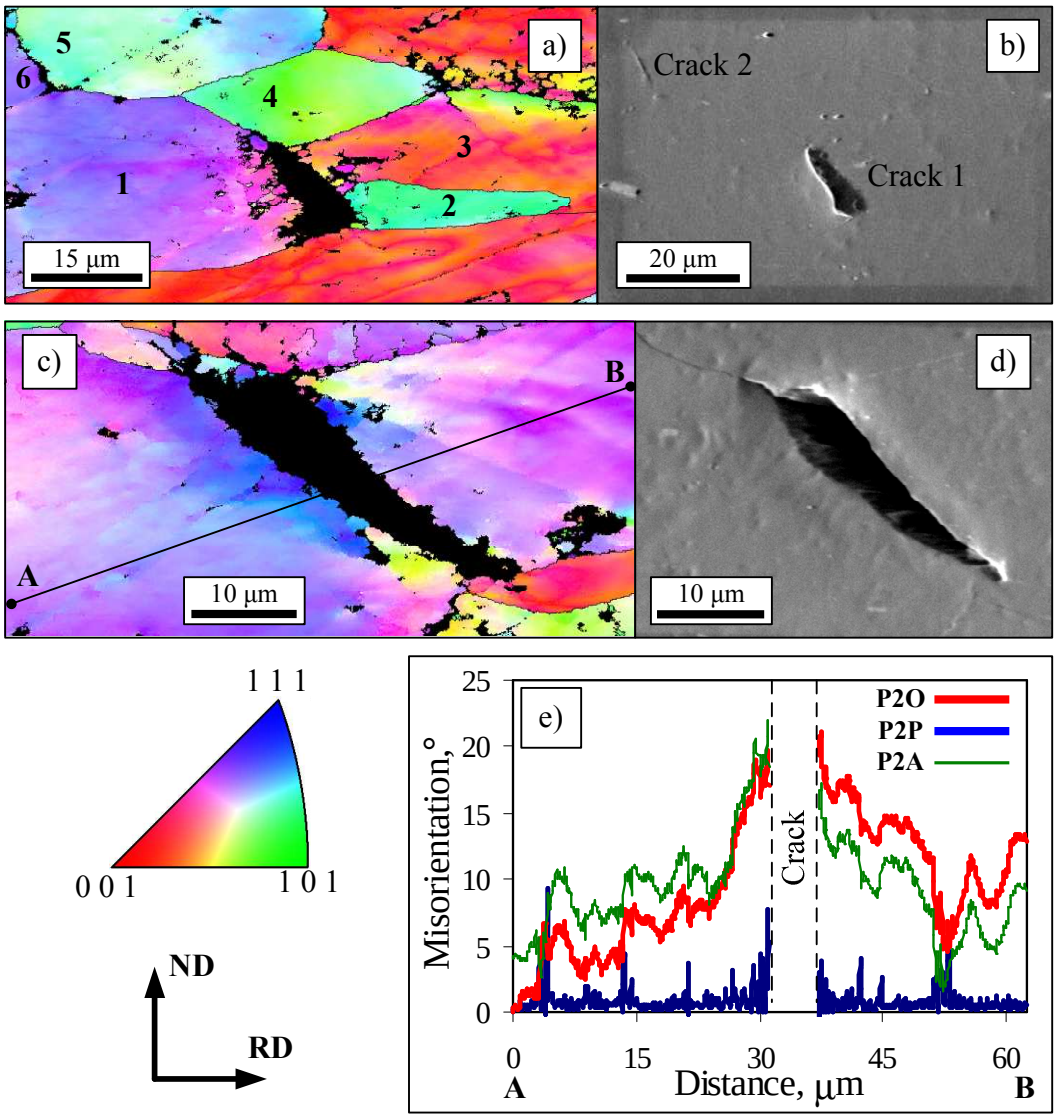

Figure 5. Inverse pole figure maps (IPF), (a) and (c), and SEM micrographs, (b) and (d), of a zone close to the fracture edge of AA6016 type 6Mg. Three different cracks are found in these maps with their origin along grain boundaries. The misorientation profile chart in (e) corresponds to the line AB traced in the IPF map of c). These curves correspond to the misorientation angle with respect to

point A (P2O), the point-to-point misorientation (P2P) and the misorientation angle with respect to the average crystal orientation considering the two adjacent grains as one.

The crack appears to be stopped in the triple junction of grains 1, 3 and 4. In the case of the crack created between grains 5 and 6, the misorientation angle is 46.7°. Grains 1 and 6 have similar orientations with a misorientation angle of 4.8° only.

A different case is observed in Fig. 5c and d where a crack is observed among two grains with similar crystal orientations. The misorientation among the average crystal orientation of both regions is 16.9° which is close to the transition value of a high to a low angle GB. A misorientation line profile along both regions (AB) was extracted from the EBSD map of Fig. 5c and is displayed in Fig. 5e. It is observed that the zones closer to the crack show an orientation gradient which can be compared from the different curves. The orientation gradient is a product of plastic deformation and shows that deformation increases in the vicinity of the crack by a gradual formation of non-redundant dislocations.

Fig. 6a and b show cracks situated between two grains in material 4Mg which form a misorientation angle of 24.4° between their average crystal orientations. This case is similar to the cracks observed on type 6Mg.

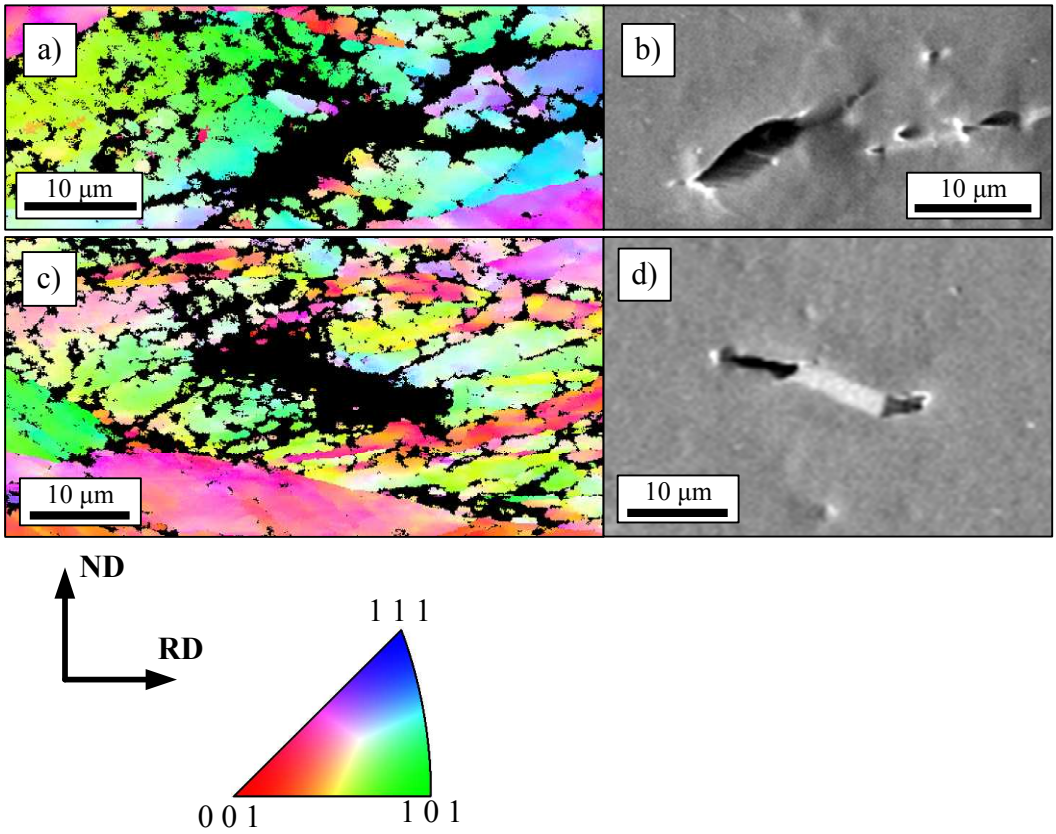

Figure 6. Inverse pole figure map (a) and SEM micrograph (b) of a zone close to the fracture edge of sample 4Mg. Both cracks which were found in these maps have their origin along grain boundaries; IPF map (c) and corresponding SEM (d) image for a crack originating at constituent particle

Fig. 6c shows an EBSD scan from a zone containing a constituent particle which is debonded from the matrix at both ends. The particle seems to be rotated towards the tensile axis and gives the impression that it tries to align itself with the elongation direction of the grain (i.e. tensile axis). The particle is found inside a grain which contains a deformation substructure with misorientation angles as high as 30°. The type of microbands observed in this grain is indicative for a strong deformation of the matrix.
The smooth orientation gradients found close to intergranular cracks suggest some deformation of the grain boundaries region before decohesion which is in agreement with the observations of Evenson et al. [2] from Laue back reflection X-ray patterns on the fracture facets.

3.4 Discussions

The SEM fractographs show some aspects of both intergranular and transgranular fracture. However, it is not possible to assert whether the void initiation has an intergranular or transgranular origin. When voids or cracks have reached a certain size, their propagation represents the next step to final failure. In this case, the propagation can also be achieved by void-sheet coalescence, which is considered as transgranular, or as intergranular if it follows the grain boundaries. Therefore, it is not possible to discriminate between the initiation and the propagation failure mechanism by only fractography. More information about the initiation mode can be obtained from broken tensile specimens by analyzing secondary voids or cracks; i.e. voids or cracks lying below fracture surface. For the secondary voids or cracks the propagation process did not extensively develop and thus the observation of 2^{ry} voids will provide information about the initiation and growth of the cavities. The use of EBSD technique to create crystal orientation maps of the regions surrounding the secondary cracks gives the advantage of both determining the origin of cracks along grain boundaries and proving the existence of deformation close to these cracks by formation of grain substructures. Therefore it can be said that cracks in both alloys occur along grain boundaries and are accompanied of plastic deformation. However, failure by dimple rupture mechanism from constituent particles is also taking place as it is observed by fractography. Initiation and growth of the voids is possible to be observed in the cross-section of the tensile samples but void coalescence could not be observed.
The intergranular failure and the dimple rupture mechanism are in competition in these alloys, although the former mechanism should be avoided due to its low energy failure process. The higher amount of cracks and the larger intergranular fracture surface area found in the aluminium alloy with higher magnesium content, type 6Mg, suggests that the intergranular mechanism increases with higher magnesium content. The action of the magnesium is not only attributed to the precipitation enrichment of the grain boundary regions but also to the hardening of the aluminium matrix by the creation of more precipitates. A harder matrix implies a larger stress on regions of plastic strain incompatibilities such as grain boundaries and a particle-matrix interface. It is believed that local stresses along grain boundaries reach a critical value which triggers the separation.

4. Conclusions

The study of the void formation during fracture of the AA6XXX alloys with variable Mg content displayed that the Mg content affects mechanical properties of the aluminium matrix. The increase of magnesium content increases the tensile strength and the microhardness of the alloy. However the strengthening of the matrix is accompanied with a decrease in the ductility. Based on the assessment of the fracture surface and secondary cracks, it was demonstrated that the higher magnesium content increases the regions of intergranular ductile failure and the number of cracks occurring along grain boundaries. Nevertheless some regions also failed by void initiation, growth and coalescence of constituent particles. This transition is attributed to the segregation of grain boundary precipitates and additionally to the high level of local stresses on grain boundaries as a consequence of the matrix strengthening.

Acknowledgements

This research was carried out under project number MC5.05220 in the framework of the Research Program of the Materials innovation institute M2i (www.m2i.nl), the former Netherlands Institute for Metals Research. The authors also acknowledge the fruitful discussions with Petar Ratchev (Aleris), Toni Chezan (Corus IJmuden) and Lin Zhuang (Corus IJmuden).

References

[1] W. S. Miller, L. Zhuang, J. Bottema, A. J. Wittebrood, P. De Smet, A. Haszler and A. Vieregge, Recent development in aluminium alloys for the automotive industry, *Materials Science and Engineering*, A280, (2000), 37- 49

[2] J. D. Evensen, N. Ryum and J. D. Embury: The Intergranular Fracture of Al-Mg-Si Alloys, *Materials Science and Engineering*, Vol. 18, (1975), 221-229

[3] K. Horikawa, S. Kuramoto and M. Kanno, Intergranular fracture caused by trace impurities in an Al-5.5 mol% Mg alloy, Acta materialia, 49, (2001), 3981-3989.

[4] S. F. Corbin, E. Ansah-Sam and D. J. Lloyd, Comparing the influence of Mn and Fe content on the fracture of a AA6XXX series alloy in different aged states, *Materials Science Forum*, Vols. 519-521, (2006), 125-130

[5] S.E. Urreta, F. Louchet, A. Ghilarducci, Fracture behaviour of an Al–Mg–Si industrial alloy, Materials Science and Engineering A302 (2001) 300–307.

[6] A. Chennakesava and S. Sundar, influence of Ageing, inclusions and voids on ductile fracture mechanism in commercial Al-alloys, *Bull. Mater. Sci*, Vol 28, No. 1, February 2005, 75-79

[7] J. Sarkar, T. R. G. Kutty, D. S. Wilkinson, J. D. Embury and D. J. Lloyd: Tensile properties and bendability of T4 treated AA6111 aluminum alloys, *Materials Science and Engineering*, A369, (2004), 258–266

[8] C. H. Caceres, C. J. Davidson, J. R. Griffiths and Q. G. Wang, The effect of Mg on the microstructure and mechanical behavior of Al-Si-Mg casting alloys, Metallurgical and Materials Transactions, 30A, October, 1999-2611

[9] K. Spencer, S. F. Corbin and D. J. Lloyd: *Materials Science and Engineering*, A325, (2002), 394–404

[10] N. Ryum, The Influence of a Precipitate-Free zone on the mechanical properties of an Al-Mg-Zn alloy, Acta Metallurgica, Vol. 16, March 1968, 327-332

[11] M. de Haas, J. Th. m. de Hosson, On the effects of thermomechanical processing on failure mode in precipitation-hardened aluminium alloys, Journal of materials science, 37, (2002), 5065 – 5073

[12] ASTM standard E 8M-97, Standard test methods for Tension Testing of Metallic Materials [Metric], Annual book of ASTM standards, 1997, 77-97